Journal of Applied Polymer Science

Light scattering materials with tunable optical properties by controlling refractive index of the dispersed phase

Xiao Liu, Xianming Dong, Ying Xiong, Ping Yi, Yikun Ren, Shaoyun Guo
The State Key Laboratory of Polymer Materials Engineering, Polymer Research Institute of Sichuan University, Chengdu 610065, China
Correspondence to: Y. Xiong (E-mail: xiongying@scu.edu.cn) and S. Guo (E-mail: nic7702@scu.edu.cn)

ABSTRACT: Traditionally, the morphologies of the dispersed phase in Polycarbonate (PC)/poly(styrene-co-acrylonitrile) (SAN) blends were strongly influenced if AN content in SAN changed significantly even under constant processing conditions. This would hinder the pure research intended to study the effect of the refractive index difference between the polymer host and the polymeric dispersed particles on the optical properties tough. Therefore, we respectively prepared different PC/SAN light diffusion sheets with four types of SAN containing different AN content ranging just from 20 to 25 wt %, a narrow range that sufficiently ensures the relatively stable morphology of different SAN in PC matrix. The results suggest that the refractive index of SAN increases with an decreasing AN content, thus narrowing the refractive index difference between PC and SAN and producing PC/SAN(70/30) light diffusion sheets with an increasing transmittance and decreasing haze. The interesting phenomenon is further analyzed using Mie scattering theory. © 2016 Wiley Periodicals, Inc. J. Appl. Polym. Sci. **2016**, *133*, 44156.

KEYWORDS: blends; light scattering; optical properties; polyesters

Received 26 March 2016; accepted 27 June 2016
DOI: 10.1002/app.44156

INTRODUCTION

Optical diffusers are widely used in artificial lightings, illuminated sign, automotive dashboards, liquid crystal displays, and so forth, to improve the brightness uniformity on the displays.[1] Traditionally, inorganic additives or organic particles like silica (SiO_2),[2] titanium dioxide (TiO_2),[3] polysiloxane, core-shell particles,[4] and ordinary polymer blends such as poly(ethylene terephthalate),[5] ethylene–vinyl acetate,[6] and poly(styrene-co-acrylonitrile) (SAN),[7–9] are commonly incorporated into polymer matrix to prepare optical diffusers with excellent transmittance and high haze.

Particle sizes, amount of dispersed phase, surface structure of the optical devices, and particle refractive index relative to the polymer host have significant effects on the spreading of transmitted light, and extensive studies have focused on tailoring these physical parameters to improve transmittance, light diffusion properties, and other optical performances.[2,10–14] Our previous work also showed that the transmittance and haze of Polycarbonate (PC)/SAN light diffusion sheets increase simultaneously with the increase of SAN mass fraction.[9] Other than modifying particle size and additives concentration, a growing amount of attentions have been paid on tailoring the materials' refractive index to control the optical properties.[14–16] Generally, the modulation of the refractive index is achieved through manipulating the structures or the constituent of the hybrid materials.[17–21] However, the above method inevitably causes micro-morphological changes to the tested materials, which would affect certain optical performances, thus reducing the validity of the result that is originally intended to link the optical properties with the refractive index difference between the polymer host and the polymeric dispersed particles.

Refractive index modulation has been a key technology in optical communication devices such as polymeric waveguides and optical diffuser. Our previous work has confirmed that PC70/SAN30 light diffusion sheets exhibit high transmittance (89.1%) and high haze (91.7%).[8] Commercially available for many years, SAN is copolymerized by styrene (St) and AN. Because the monomers and homopolymer of St and AN have different refractive index, the refractive index of SAN can be easily tuned by controlling the AN contents, and the phase morphology of PC/SAN blends as a function of AN content in SAN has been extensively investigated.[22–24] However, it appears that the obtained morphologies of the dispersed phase in PC/SAN blends are strongly influenced by changes in AN mass fraction range under the same processing conditions. Therefore, this article investigates the effect of the refractive index difference between PC and SAN on the optical properties of the PC70/SAN30 optical diffuser under variable AN contents ranging

Table I. Polymers Used in This Study

Polymer	Source	Commercial description	Density (g/cm^3)
PC	LG DOW Polycarbonate Ltd.	201-22	1.20
SAN1	Chi Mei Co.	PN-107	1.06
SAN2	Formosa Plastic (Ningbo) Ltd.	NF-2200	1.06
SAN3	Chi Mei Co.	PN-117	1.06
SAN4	Chi Mei Co.	PN-106	1.06

from 20 to 25 wt %. Because the AN mass fraction range is narrow, the average particle sizes and particle size distributions of the four types of SAN in PC are controlled to be approximately the same. As a result, the interference of the morphological variation in optical properties would be eliminated.

EXPERIMENTAL

Materials and Preparation of Light Diffusion Sheets

The characteristics of the polymers used in this work are demonstrated in Table I. The raw materials were first dried under vacuum for 24 h at 80 °C, and then 70 wt % PC and 30 wt % SAN with various AN-contents were melt mixed at 240 °C for 5 min in a HAAKE PolyLab QC machine respectively, with the rotor speed fixed at 30 rpm for the preparation of all blends. Then, sample light diffusion sheets with a thickness of 0.60 mm were prepared by compression molding at a temperature of 240 °C with the blends obtained above.

Transmittance and Haze

Transmittance (T) and haze (H) are defined as stated by ASTM D1003-61 with a Transmittance-Haze testing instrument (WGT-S, Shanghai Precision and Scientific Instrument Corporation, China). According to ASTM D1003-61, haze is the percent of transmitted light that is scattered so that its direction deviates more than 2.5° from the direction of the incident beam.[25] As shown in Figure 1, all transmitted light within the hemisphere scope can be trapped using the integrating sphere. Haze and transmittance data are especially useful for quality control and specification purposes.[26] They can be written as

$$T = \frac{I_t}{I_0} \tag{1}$$

$$H = \frac{(I_t)_{2.5}^{90}}{I_t} \tag{2}$$

where I_t is the intensity of the transmitted light, I_0 the intensity of the incident light and $(I_t)_{2.5}^{90}$ the intensity of the part of transmitted light with scattering angle more than 2.5° while passing through the sample.

Scanning Electron Microscope

The size of the dispersed phase and the morphology of the PC/SAN light diffusion sheet were examined by scanning electron microscopy (SEM, FEI, Netherlands). SEM samples were immersed in liquid nitrogen for 1 h and then brittle fractures were performed. The fracture surfaces were coated with a layer of gold in a vacuum chamber for conductivity. For the micrographs, the particles were traced by hand, and the manual trace was instantaneously scanned into the Nano-measurer, a particle size analysis software that automatically detected the edges of the particles. Thus, the diameters of the particle were calculated by the software itself. To determine the average particle size of the dispersed phase, at least 300 cross sections of the dispersed particles of each sample were counted.

Element Analysis and Refractive Index Measurement

Nitrogen (N) content in SAN was determined by a CHNS/O elemental analyzer (EA, EUROVECTOR EA3000, Italy) with 100 ppm–100%. Refractive index (n) was measured using an Abbe refractometer (WYA (2WAJ), $\lambda = 589.3$ nm, 20 °C) from Shanghai Precision and Scientific Instrument Corporation. Samples with a smooth flat surface were prepared by compression molding at 240 °C.

RESULTS AND DISCUSSION

Optical Properties

Photographs in Figure 2 captured the school badge and text characters clearly observed under a PC/SAN1 light scattering sheet, which testified its evident capacity to act as an optical diffuser because of the highly perceptible transparency and object size.

Figure 3 shows the transmittance and haze of the PC/SAN light diffusion sheets with four different SAN, indicating that all samples have transmittance higher than 87.5% and haze higher than 87.0%, good enough for the light diffusion sheets to be applied in polymeric waveguides and optical diffusers. Conversely, although the composition of the blend and processing condition were fixed, as introduced in Materials and Preparation of Light Diffusion Sheets section, the light diffusion sheets displayed different optical properties, in which PC/SAN4 have the highest transmittance and the lowest haze. The light diffusion sheet samples exhibited increasing transmittance and decreasing haze as its SAN code varying from SAN1 to SAN4, a

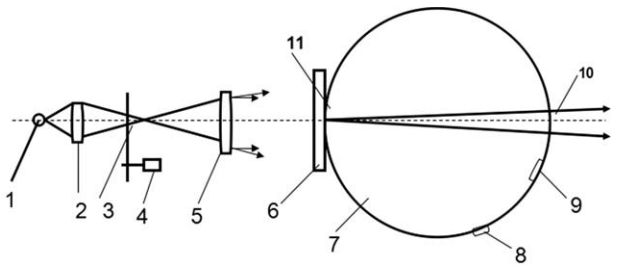

Figure 1. Optical system of the Transmittance-Haze testing instrument: (1) Source, (2) Condenser, (3) Aperture, (4) Modulator, (5) Lens, (6) Sample, (7) Integrating sphere, (8) Photocell, (9) Reflectance Standard, (10) Emergent Window, and (11) Entrance Window.

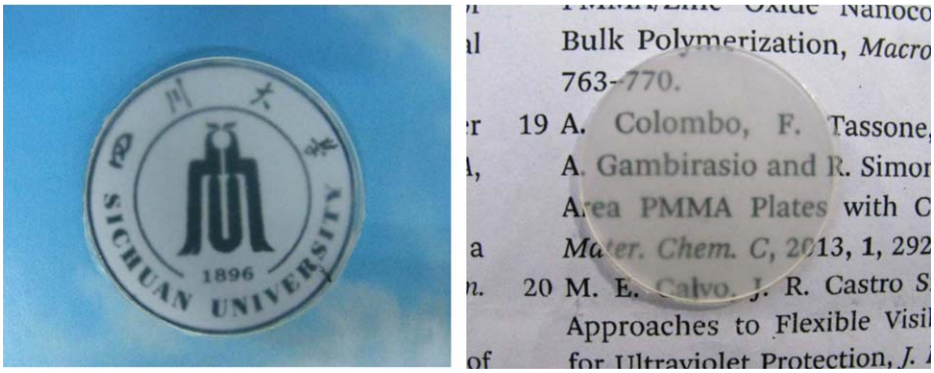

Figure 2. Photographs of the image (left) and characters (right) behind the PC/SAN1 light scattering sheets. [Color figure can be viewed in the online issue, which is available at wileyonlinelibrary.com.]

regular pattern that we will discuss through various characterization methods such as SEM, EA, and refractive index analysis.

SEM Analysis

As the morphology and the particle sizes of the dispersed phase produce significant spreading of the transmitted light, the structure of the brittle fractures of PC/SAN sheets was examined by SEM. Noted in Figure 4, four types of SAN, all of which are spherical particles different from the ill-defined circular domains obtained in other studies,[22] dispersed uniformly in PC matrix. Particle sizes of the dispersed phase of the four samples were analyzed using Nano-measurer, with at least 300 cross sections of the dispersed particles counted, to figure out if particle size (of 4 SANs) is responsible for the distinction of optical properties of PC sheets containing the same content but different SAN domains. The average diameter (d) can be calculated by the following equation

$$d = \frac{\sum_{i=1}^{N} n_i d_i}{\sum_{i=1}^{N} n_i} \tag{3}$$

where, n_i represents the number of the particles with a diameter of d_i. The calculated results show that the average diameters of specimens are 2.41, 1.90, 2.79, and 2.07 μm, respectively, with minimal fluctuations around 2.00 μm. In addition, the standard deviations of SAN particles for the samples PC/SAN1, PC/SAN2, PC/SAN3, PC/SAN4 are 1.93, 1.71, 1.87, 1.85 in sequence, which are very close to each other. Hence, particle sizes and particle size distributions of the SAN domains are not the main factor that contributes to the variation of the optical properties of PC sheets containing different SAN.

EA and Refractive Index Analysis

As the relatively constant particle size of four types of SAN in PC is not the main factor responsible for the distinct optical properties of the PC/SAN light diffusion sheets with different SAN, so that we naturally take the refractive index discrepancy between PC and different SAN into account. The refractive indices of the four types of SAN were measured by an Abbe refractometer ($\lambda = 589.3$ nm), and elemental analysis was used to determine the nitrogen (N) content, thus the AN content which has a dominant influence on the final refractive index of each SAN copolymer. AN content is calculated according to eq. (4),

$$C_{AN} = \frac{C_N * M_{C_3H_3N}}{M_N} \tag{4}$$

where C_{AN} is the AN content in SAN, C_N the N content in SAN, $M_{C_3H_3N}$ the molar mass of Acrylonitrile molecule and M_N the molar mass of Nitrogen atom. AN content and refractive indices of SAN are listed in Table II, showing that the AN content gradually decreased from 25.7 wt % to 20.9 wt %, a narrow range that sufficiently ensures the relatively stable morphology of different SAN in PC matrix, and this trend corresponds to the results displayed in Figure 4. Figure 5 shows the refractive index as a function of AN content in SAN. It is easily concluded that the refractive index of SAN increases as AN content decreases. The refractive index depends on the molecular volume, and Naoki Yasuda et al. controlled the refractive index of the silicone ladder polymer films to be between 1.555 and 1.466 by changing the vinyl group content.[27] It makes sense that the refractive index of SAN lies between PS (1.5894) and PAN(1.5187) because SAN is copolymerized by styrene (St) and AN, whose monomers and homopolymer have different refractive indices. In addition, the refractive index will increase with a decrease of AN content in the copolymer. Therefore, the SAN refractive index can be easily tuned by controlling the AN contents.

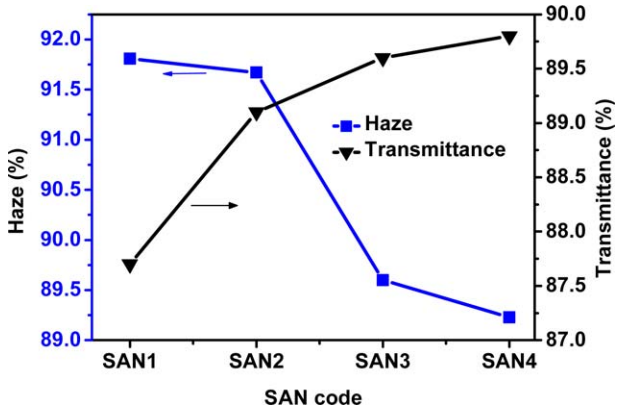

Figure 3. Transmittance and haze of the PC70/SAN30 light diffusion sheets with four different SAN. [Color figure can be viewed in the online issue, which is available at wileyonlinelibrary.com.]

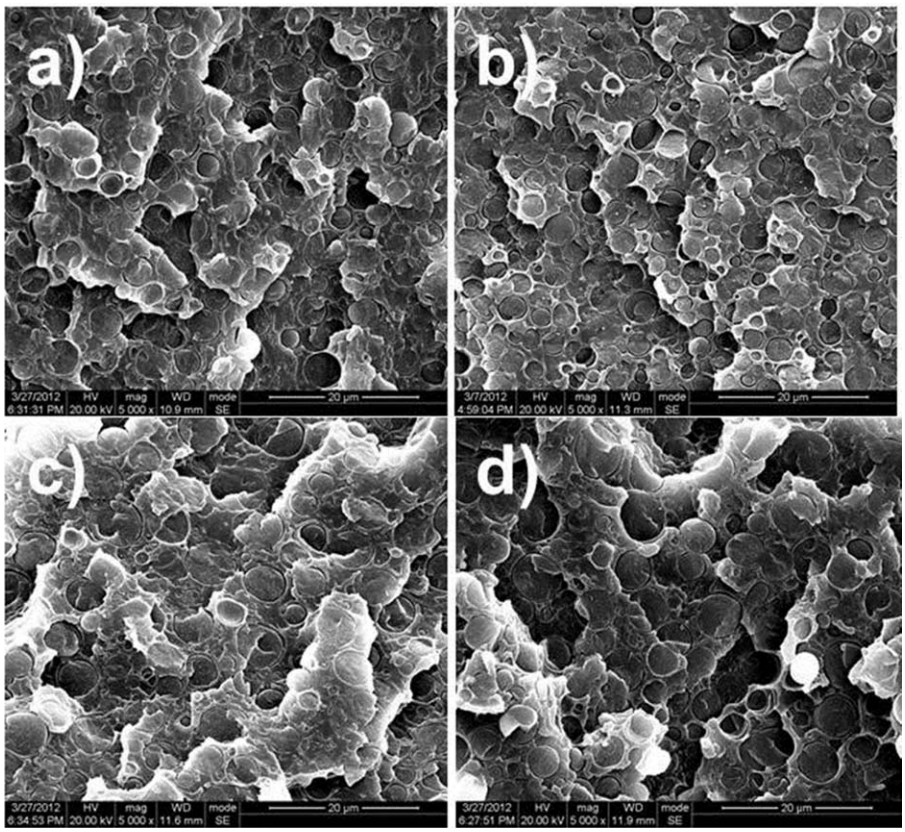

Figure 4. SEM pictures of PC70/SAN30 specimens for different SAN. (a) PC/SAN ($d = 2.41$ μm), (b) PC/SAN2 ($d = 1.90$ μm), (c) PC/SAN3 ($d = 2.79$ μm), and (d) PC/SAN4 ($d = 2.07$ μm).

Mie Scattering Theory

The refractive index of pure PC is 1.5832. It is defined that m is the relative refractive index between scattering particle (n_2) and matrix (n_1)

$$m = n_2/n_1 = 1+\mu \tag{5}$$

where μ can be either positive or negative depending on the relative refractive index between dispersed phase and matrix. Here, we use the absolute value $|\mu|$ to represent the relative difference of refractive index between SAN and PC. The calculated parameters of each specimen are listed in Table III. Figure 6 shows an increase of transmittance and a decrease of haze with the decreasing $|\mu|$, suggesting that the relative refractive index between scattering particles and matrix plays an important role in the optical performance. Then, what is the best value of $|\mu|$ to achieve the optimal diffusion effect?

The value of T^*H, the product of the transmittance and the haze, were often used to measure the light scattering cabability of optical materials.[28,29] According to eqs. (1) and (2), T^*H equals to $\frac{(I_t)_{2.5}^{90}}{I_0}$, namely the ratio of the forward scattered light with a direction deviating more than 2.5° to the incident light,

Table II. Composites and Refractive index of SAN Used in This Study

Polymer	N content (wt %)	AN content (wt %)	Refractive index
PC	/	/	1.5832
SAN1	6.79	25.7	1.5669
SAN2	6.74	25.5	1.5686
SAN3	6.29	23.8	1.5700
SAN4	5.52	20.9	1.5720

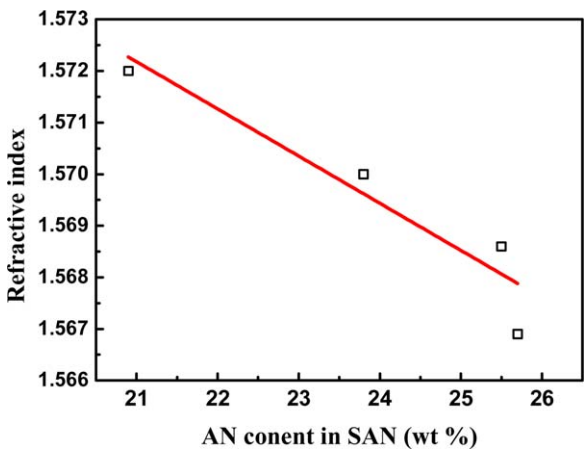

Figure 5. The refractive index of SAN as a function of AN content in SAN. [Color figure can be viewed in the online issue, which is available at wileyonlinelibrary.com.]

Table III. Parameters of SAN Particles for Different Specimens

Specimen	*m*	| μ |	*d* (μm)
PC/SAN1	0.9897	0.0103	2.41
PC/SAN2	0.9908	0.0092	1.90
PC/SAN3	0.9917	0.0083	2.79
PC/SAN4	0.9929	0.0071	2.07

similar to the diffusive transmittance introduced in another paper.[30] The peak value of T^*H, instructive to the preparation of light scattering sheets, occurs when $|\mu|$ is about 0.009. It should also be noted that at larger *m*, stronger backscattering appears; consequently, to obtain a light-diffusing film with more forward scattering, it is necessary to set m close to 1. However, as the difference in refractive index between the particles and matrix becomes smaller, the amount of directly transmitted light increases.[11] Therefore, an optimal value of $|\mu|$ exists for certain systems, and the value of μ should be determined in consideration of particle size and mass fraction of the dispersed phase.[11,13]

The scattering characteristics of a spherical particle with arbitrary size and refractive index and the effect of relative refractive index on the optical properties can be analyzed by Mie scattering theory.[31,32] For the sake of simplicity, we assume that the dispersed particles have the same, average diameters of 2.00 μm in this study.

Figure 7 shows that every single particle scatters the incident light as a scattering unit in the scattering sheet. Within the sheet, there is an uneven distribution of various refractive indices, and scatterings occur as a result of the mismatch of these refractive indices. The transmitted lights consist of the direct light and the scattered light. According to Mie scattering theory,[31,32] the scattering light intensity profile of a particle can be calculated as follows:

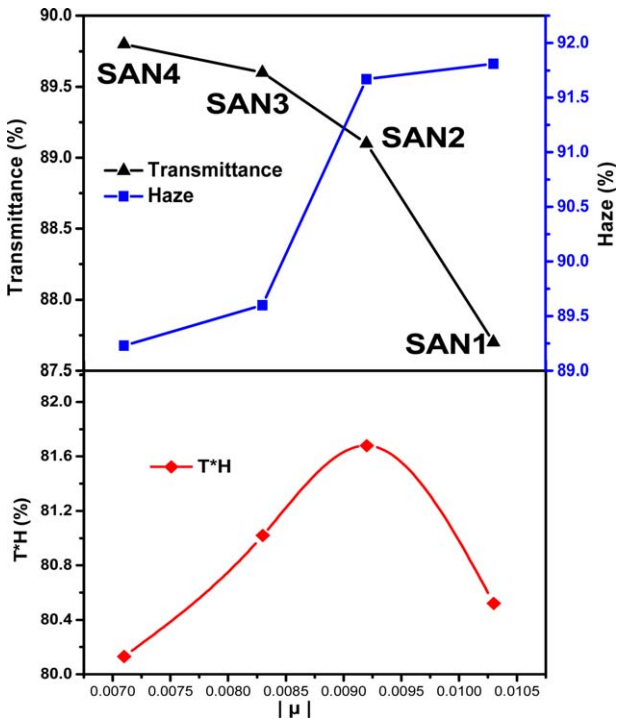

Figure 6. Effect of | μ | on the transmittance and haze (top) and T^*H (bottom) of PC light scattering sheet. [Color figure can be viewed in the online issue, which is available at wileyonlinelibrary.com.]

$$I=\frac{\lambda^2}{8\pi^2 r^2} I_0(i_1+i_2) \tag{6}$$

$$i_1=s_1(\mathrm{m},\theta,\alpha)\times s_1^*(\mathrm{m},\theta,\alpha) \tag{7}$$

$$i_2=s_2(\mathrm{m},\theta,\alpha)\times s_2^*(\mathrm{m},\theta,\alpha) \tag{8}$$

$$s_1=\sum_{n=1}^{\infty}\frac{2n+1}{n(n+1)}(a_n\pi_n+b_n\tau_n) \tag{9}$$

$$s_2=\sum_{n=1}^{\infty}\frac{2n+1}{n(n+1)}(a_n\tau_n+b_n\pi_n) \tag{10}$$

$$b_n=\frac{m\phi_n(\alpha)\phi_n'(m\alpha)-\phi_n'(\alpha)\phi_n(m\alpha)}{m\xi_n(\alpha)\phi_n'(m\alpha)-\xi_n'(\alpha)\phi_n(m\alpha)} \tag{11}$$

$$a_n=\frac{\phi_n(\alpha)\phi_n'(m\alpha)-m\phi_n'(\alpha)\phi_n(m\alpha)}{\xi_n(\alpha)\phi_n'(m\alpha)-m\xi_n'(\alpha)\phi_n(m\alpha)} \tag{12}$$

$$\pi_n=\frac{dp_n(\cos\theta)}{d(\cos\theta)} \tag{13}$$

$$\tau_n=\frac{d}{d\theta}p_n^{(1)}(\cos\theta) \tag{14}$$

$$f_n(z)^n=\left(\frac{z\pi}{2}\right)^{1/2}J_{n+\frac{1}{2}}(z) \tag{15}$$

$$\xi_n(z)^n=\left(\frac{z\pi}{2}\right)^{1/2}H_{n+\frac{1}{2}}^{(2)}(z) \tag{16}$$

$$a=n_1\pi d/\lambda \tag{17}$$

$$m=n_2/n_1 \tag{18}$$

$$k=\frac{2}{a^2}\sum_{i=1}^{N}(2n+1)\ \left(|a_n|^2+|b_n|^2\right) \tag{19}$$

Here, λ is the incident wavelength, r is the distance from the center of the sphere, d is the diameter of the sphere, θ is the scattering angle, I_0 is the intensity of the incident light (watt/m^2), m is the relative refractive index between particle (n_2) and matrix (n_1), α is the size parameter, and k is the scattering coefficient. $\varphi_n(z)$ and $\zeta_n(z)$ are the Ricatti-Bessel functions, $\varphi'(\alpha)$ is the derived fucnction of $\varphi(\alpha)$, and $P_n(\cos\theta)$, $P_n^{(1)}(\cos\theta)$ are Legendre and associated Legendre functions of $\cos\theta$, respectively.

If all the spherical particles have the same size with an amount of concentration c, the total scattering section per unit volume Q would be

$$Q=\mathrm{ck}\frac{\pi d^2}{4} \tag{20}$$

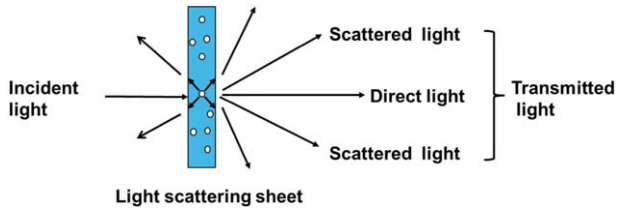

Figure 7. Schematics of structure of light scattering sheet and light scattering by a single particle. [Color figure can be viewed in the online issue, which is available at wileyonlinelibrary.com.]

Q represents the scattered probability of the incident light, and the larger the Q value, the larger the probability of the light being scattered.

According to eq. (17), the value of size parameter α is 18.1($n_1 = 1.5832$, $d = 2000$ nm, $\lambda = 550$ nm). The relative values of each calculated Q are Q_1:Q_2:Q_3:Q_4 = 2.1:1.7:1.4:1.0, showing an decreasing tendency. That is to say, the scattering probability decreases as the relative difference of refractive index decreases, leading to a decreasing haze value. Low scattering probability brings about less multi-scattering within the material and reduced reflectance, as a result, the transmittance increases with the refractive index match of the matrix and the dispersed phase.

CONCLUSIONS

In this work, the refractive index of the dispersed phase is controlled to fabricate and characterize PC/SAN optical diffuser with adjustable optical performance. Despite the unstable morphologies of the dispersed phase in PC/SAN blends under constant processing condition yet significant change in AN mass fraction of SAN, we respectively prepared different PC/SAN light diffusion sheets with four types of SAN, each with a distinct AN content ranging from 20 to 25 wt %, a narrow range that sufficiently ensures the relatively stable morphology of different SANs in PC matrix. As a result, the effect of the particle size of SAN on the optical properties can be eliminated, enabling the pure research of the effect of relative refractive index of polymeric dispersed particles to the polymer host on the optical properties of PC/SAN optical diffuser. The results show that the refractive index of SAN increases with a decrease in AN content, thus narrowing the refractive index difference between PC and SAN and producing PC/SAN(70/30) light diffusion sheets with an increasing transmittance, due to a lower intensity of backscattering, and a decreasing haze, due to a decreased total scattering section per unit volume according to Mie scattering theory. Additionally, the peak value of T^*H, the product of the transmittance and the haze, occurs when the refractive index difference between the matrix and the dispersed phase equals about 0.009. The optimization bears great significance and practical value in refractive index modulation, a key technology in optical communication devices such as polymeric waveguides and optical diffuser.

ACKNOWLEDGMENTS

The research is financed the Key Scientific and Technical Support Program of Sichuan Province under grant no. 2014GZ0031, the Applied Basic Research Program of Sichuan Province under grant no. 2016JY0229 and the National Natural Science Foundation of China under grant no. 51227802.

REFERENCES

1. Colombo, A.; Tassone, F.; Santolini, F.; Contiello, N.; Gambirasio, A.; Simonutti, R. *J. Mater. Chem. C* **2013**, *1*, 2927.
2. Shin, K.; Kim, H. N.; Cho, J. C.; Moon, S. J.; Kim, J. W.; Suh, K. D. *Macromol. Res.* **2012**, *20*, 385.
3. Yuwono, A. H.; Xue, J. M.; Wang, J.; Elim, H. I.; Ji, W.; Li, Y.; White, T. J. *J. Mater. Chem.* **2003**, *13*, 1475.
4. Small, A.; Hong, S.; Pine, D. *J. Polym. Sci. Polym. Phys.* **2005**, *43*, 3534.
5. Liu, X.; Xiong, Y.; Shen, J.; Guo, S. *Opt. Express* **2015**, *23*, 17793.
6. Luo, S.; Yi, P.; Xiong, Y.; Shen, J.; Guo, S. *J. Appl. Polym. Sci.* **2015**, *133*, DOI: 10.1002/app.42844.
7. Dong, X. M.; Xiong, Y.; Chen, G. S.; Guo, S. Y. *Appl. Opt.* **2015**, *54*, 608.
8. Dong, X.; Xiong, Y.; Ren, Y.; Xue, J.; Chen, F.; Guo, S. *Acta Polym. Sin.* **2013**, *13*, 241.
9. Yi, P.; Xiong, Y.; Guo, S. *Appl. Opt.* **2015**, *54*, 10000.
10. Jonsson, J. C.; Karlsson, L.; Nostell, P.; Niklasson, G. A.; Smith, G. B. *Sol. Energy Mater. Sol. Cells* **2004**, *84*, 427.
11. Ishinabe, T.; Nakayama, T.; Miyashita, T.; Uchida, T. *Jpn. J. Appl. Phys.* **2004**, *43*, 6152.
12. Hu, J.; Zhou, Y.; Sheng, X. *J. Mater. Chem. C* **2015**, *3*, 2223.
13. Smith, G. B.; Jonsson, J. C.; Franklin, J. *Appl. Opt.* **2003**, *42*, 3981.
14. Schulz, H.; Burtscher, P.; Mädler, L. *Compos. Part A* **2007**, *38*, 2451.
15. O'Brien, D. J.; Chin, W. K.; Long, L. R.; Wetzel, E. D. *Compos. Part A* **2014**, *56*, 161.
16. Zhou, R. J.; Burkhart, T. *J. Appl. Polym. Sci.* **1866**, *115*, 2010.
17. Walheim, S.; Schaffer, E.; Mlynek, J.; Steiner, U. *Science* **1999**, *283*, 520.
18. Lee, C. R.; Lin, S. H.; Guo, C. H.; Chang, S. H.; Mo, T. S.; Chu, S. C. *Opt. Express* **2010**, *18*, 2406.
19. Ibn-Elhaj, M.; Schadt, M. *Nature* **2001**, *410*, 796.
20. Cho, A. R.; Park, S. Y. *Opt. Mater. Express* **2015**, *5*, 690.
21. Griesser, T.; Höfler, T.; Jakopic, G.; Belzik, M.; Kern, W.; Trimmel, G. *J. Mater. Chem.* **2009**, *19*, 4557.
22. Hanafy, G. M.; Madbouly, S. A.; Ougizawa, T.; Inoue, T. *Polymer* **2004**, *45*, 6879.
23. Hyuk Jin, J.; Younggon, S.; Park, O. O. *Macromol. Res.* **2014**, *22*, 146.

24. Li, H. G.; Yang, Y.; Fujitsuka, R.; Ougizawa, T.; Inoue, T. *Polymer* **1999**, *40*, 927.

25. Tenma, M.; Mieda, N.; Takamatsu, S.; Yamaguchi, M. *J. Polym. Sci. Polym. Phys.* **2008**, *46*, 41.

26. Bafna, A.; Beaucage, G.; Mirabella, F.; Skillas, G.; Sukumaran, S. *J. Polym. Sci. Polym. Phys.* **2001**, *39*, 2923.

27. Yasuda, N.; Yamamoto, S.; Minami, S.; Nobutoki, H.; Wada, Y.; Yanagida, S. *Jpn. J. Appl. Phys.* **2002**, *41*, 624.

28. Xin, L.; Zhong, X. *J. Chem. Ind. Eng.* **2006**, *4*, 45.

29. Wenshi, M.; Yu, D.; Hong, W.; Yingbin, X. *Polym. Mater. Sci. Eng.* **2012**, *8*, 031.

30. Marek, M.; Steidl, J. *J. Mater. Sci.* **2006**, *41*, 3117.

31. Dang, A.; Ojha, S.; Hui, C. M.; Mahoney, C.; Matyjaszewski, K.; Bockstaller, M. R. *Langmuir* **2014**, *30*, 14434.

32. Bohren, C. F.; Huffman, D. R. *Absorption and Scattering of Light by Small Particles;* Wiley, **1983**; p 82.